SUPPORTING INFORMATION: Correlation between thermophoretic behavior and hydrophilicity for various alcohols

Monika Bjelčić, Doreen Niether and Simone Wiegand

May 23, 2019

Contents

S1 Properties of the investigated alcohols

In this short paragraph we summarize some properties of the investigated alcohols, which might be helpful to compare the results as the sequence of the diffusion coefficients in relation to the molar mass as displayed in Fig. 3 in the main manuscript.

Table S1: List of investigated alcohols with a partial chemical formula, molecular mass in g/mol, calculated van der Waals volume V_{vdW} in $\mathrm{cm}^3/\mathrm{mol}$ [2] and $\log P$.

alcohol	partial chemical formula	M_w	V_{vdW}	$\log P$
methanol	CH_3OH	32.04	22	−0.57
ethanol	CH_3CH_2OH	46.07	32	−0.22
1-propanol	$CH_3CH_2CH_2OH$	60.10	42	0.25
ethylene glycol	$OHCH_2CH_2OH$	62.07	37	−1.31
propylene glycol	$CH_3COH_2CH_2OH$	76.09	47	−0.9
propane-1,3-diol	$OH[CH_2]_3OH$	76.10	47	−1.26
butane-1,4-diol	$OH[CH_2]_4OH$	90.12	57	−0.81
glycerol	$OHCH_2COH_2CH_2OH$	92.02	51	−1.98
arabitol	$OHCH_2[OHCH]_3CH_2OH$	152.15	81	−3.33
mannitol	$OHCH_2[OHCH]_4CH_2OH$	182.17	96	−4

S2 Refractive index contrast factors

S2.1 Refractive index contrast measurements

The refractive index increments with temperature $(\partial \mathrm{n}/\partial \mathrm{T})_{\mathrm{p,c}}$ were measured interferometrically [3]. Measurements were performed for all concentrations measured by IR-TDFRS, around temperatures across the temperature range between 10-60°C for all with maximum heating rate of 2 mK/sec. The refractive index increments with temperature $(\partial \mathrm{n}/\partial \mathrm{T})_{p,c}$ for 1-propanol and ethane-1,2-diol are listed in the table S2 and S3, respectively. Additionally, you find the data for propane-1,2-diol, propane-1,3-diol and butane-1,4-diol in water Table S4 and for aqueous solutions of glycerol, arabitol and mannitol in Table S5.

Table S2: Refractive index increments with temperature $(\partial n/\partial T)_{p,c}$ of 1-propanol in water. Concentration c in the mass fraction of 1-propanol.

	$(\partial n/\partial T)_{p,c}/10^{-4}\mathrm{K}^{-1}$				
$T/°\mathrm{C}$ \ c/wt	0.2045	0.258	0.464	0.653	0.868
10	−1.92	−2.29	−2.97	−3.43	−3.89
20	−2.11	−2.41	−3.06	−3.52	−3.97
30	−2.28	−2.52	−3.15	−3.62	−4.06
40	−2.44	−2.64	−3.25	−3.72	−4.17
50	−2.58	−2.75	−3.36	−3.83	−4.28
60	−2.72	−2.88	−3.48	−3.95	−4.41
70	−2.85	−3.00	−3.61	−4.07	−4.55

Table S3: Refractive index increments with temperature $(\partial n/\partial T)_{p,c}$ of ethane-1,2-diol in water. Concentration c in the mass fraction of ethane-1,2-diol.

	$(\partial n/\partial T)_{p,c}/10^{-4}\mathrm{K}^{-1}$		
$T/°\mathrm{C}$ \ c/wt	0.272	0.5	0.703
10	−1.32	−2.01	−2.97
20	−1.53	−2.12	−3.06
30	−1.73	−2.23	−3.15
40	−1.91	−2.34	−3.25
50	−2.08	−2.45	−3.36
60	−2.24	−2.56	−3.48
70	−2.39	−2.67	−3.61

Table S4: Refractive index increments with temperature $(\partial n/\partial T)_{p,c}$ of propane-1,2-diol, propane-1,3-diol and butane-1,4-diol in water. Concentration c in the mass fraction of propane-1,2-diol, propane-1,3-diol and butane-1,4-diol.

	$(\partial n/\partial T)_{p,c}/10^{-4}\mathrm{K}^{-1}$			
	propane-1,3-diol		propane-1,2-diol	butane-1,4-diol
$T/°\mathrm{C}$ \ $c/\mathrm{wt}\%$	0.12	0.257	0.114	0.263
10	−0.71	−1.11	-0.78	-1.22
20	−1.04	−1.36	-1.11	-1.48
30	−1.33	−1.59	-1.40	-1.72
40	−1.59	−1.81	-1.66	-1.94
50	−1.81	−2.01	-1.88	-2.14
60	−2.00	−2.18	-2.06	-2.32

Table S5: Refractive index increments with temperature $(\partial n/\partial T)_{p,c}$ of glycerol, arabitol and mannitol in water. Concentration c in the mass fraction of glycerol, arabitol and mannitol.

	$(\partial n/\partial T)_{p,c}/10^{-4}\mathrm{K}^{-1}$			
	glycerol		arabitol	mannitol
$T/°\mathrm{C}$ \ $c/\mathrm{wt}\%$	0.12	0.231	0.255	0.297
10	-0.89	-1.10	-1.15	-0.81
20	-1.18	-1.34	-1.39	-1.11
30	-1.44	-1.56	-1.60	-1.38
40	-1.66	-1.76	-1.79	-1.61
50	-1.85	-1.94	-1.96	-1.82
60	-2.02	-2.10	-2.11	-1.98

S2.2 Refractive index contrasts with concentration

Refractive indices were measured for seven concentrations at the same temperature range as IR-TDFRS for each system. The refractive index increments with the mass concentration $(\partial \mathrm{n}/\partial \mathrm{c})_{\mathrm{p,T}}$ were measured by an Anton Paar RXA 156 refractometer, with an accuracy of 0.00002 nD and temperature control of $\Delta T = \pm 0.03$K. This refractometer uses a wavelength of 589.3 nm (sodium line), which is shorter than the wavelength of the read-out beam in our IR-TDFRS setup (HeNe-laser, 632.8 nm). This causes a small systematic error in the refractive index increment in the order of 0.5-1% [4, 5]. The concentration and temperature dependence of n was fitted with a function to determine $(\partial \mathrm{n}/\partial \mathrm{c})_{\mathrm{p,T}}$. Table 5 to 12 shows the measured values over the investigated temperature and concentration range.

Table S6: Refractive index n of 1-propanol in water. Concentration c in the mass fraction of 1-propanol.

	n				
$T/°\mathrm{C}$ \ c/wt	0.258	0.451	0.653	0.868	1
10	1.3574	1.36937	1.37921	1.38711	1.38931
20	1.35517	1.36636	1.37572	1.38315	1.38513
30	1.35267	1.36315	1.37205	1.37908	1.38099
40	1.3496	1.35986	1.36832	1.37488	1.37675
50	1.34645	1.35645	1.36447	1.37065	1.37245
60	1.3427	1.35275	1.3605	1.36644	1.36806
70	1.3394	1.3488	1.3566	1.36185	1.3635

Table S7: Refractive index n of butane-1,4-diol in water. Concentration c in the mass fraction of butane-1,4-diol.

	n					
$T/°\mathrm{C}$ \ c/wt	0.12	0.34	0.512	0.696	0.862	1
10	1.34505	1.37305	1.39627	1.41839	1.43792	1.44891
20	1.34414	1.37138	1.39399	1.41577	1.43385	1.44606
30	1.34289	1.36951	1.39166	1.4132	1.43109	1.44315
40	1.34136	1.36753	1.3891	1.41053	1.42804	1.44019
50	1.33962	1.36521	1.38651	1.40754	1.42536	1.43731
60	1.33782	1.36357	1.38437	1.40501	1.42258	1.43433
70	1.33577	1.36111	1.38161	1.40184	1.42012	1.43108

Table S8: Refractive index n of ethane-1,2-diol in water. Concentration c in the mass fraction of ethane-1,2-diol.

	n					
c/wt / T/°C	0.06	0.272	0.496	0.681	0.898	1
10	1.33954	1.36103	1.38491	1.4039	1.4242	1.43451
20	1.33864	1.35956	1.38287	1.40147	1.42185	1.4317
30	1.33739	1.35786	1.38059	1.39892	1.4188	1.42888
40	1.33591	1.35596	1.37826	1.39625	1.42592	1.42592
50	1.33416	1.35391	1.37577	1.39355	1.41315	1.42272
60	1.33372	1.35186	1.37337	1.39091	1.40984	1.41908
70	1.33019	1.35029	1.37215	1.38803	1.40682	1.41552

Table S9: Refractive index n of propane-1,3-diol in water. Concentration c in the mass fraction of propane-1,3-diol.

	n					
c/wt / T/°C	0.105	0.305	0.504	0.708	0.863	1
10	1.34434	1.36681	1.3899	1.41061	1.42902	1.44219
20	1.34346	1.36541	1.38796	1.40841	1.42659	1.43841
30	1.34225	1.3638	1.38579	1.40588	1.42378	1.43647
40	1.34065	1.36188	1.38343	1.40338	1.42093	1.43207
50	1.33885	1.35978	1.38098	1.40066	1.41824	1.43045
60	1.33836	1.35759	1.37857	1.39783	1.41526	1.42723

Table S10: Refractive index n of propane-1,2-diol in water. Concentration c in the mass fraction of propane-1,2-diol.

	n					
c/wt / T/°C	0.118	0.316	0.517	0.707	0.894	1
10	1.34676	1.37063	1.39363	1.41279	1.42877	1.4364
20	1.34573	1.36879	1.39112	1.40999	1.42549	1.43306
30	1.34432	1.36678	1.38844	1.40683	1.42221	/
40	1.34283	1.36475	1.386	1.40417	1.41887	1.42595
50	1.34115	1.3626	1.38341	1.40095	1.41551	1.42229
60	1.33903	1.35988	1.3804	1.39812	1.41225	1.41857

Table S11: Refractive index n of glycerol in water. Concentration c in the mass fraction of glycerol.

	n					
T/°C \ c/wt	0.133	0.309	0.462	0.658	0.895	1
10	1.35042	1.37353	1.39498	1.42458	1.45873	1.47621
20	1.34947	1.37228	1.39339	1.42257	1.45654	1.4738
30	1.34799	1.37048	1.39138	1.42024	1.45392	1.47103
40	1.34635	1.36849	1.38918	1.41774	1.45113	1.46687
50	1.34451	1.36642	1.38685	1.41553	1.44849	1.46094
60	1.34257	1.3643	1.38447	1.41287	1.44579	1.45774

Table S12: Refractive index n of arabitol in water. Concentration c in the mass fraction of arabitol.

	n								
T/°C \ c/wt	0.053	0.097	0.155	0.196	0.254	0.304	0.351	0.388	0.447
10	1.34169	1.34793	1.35667	1.3637	1.37204	1.38041	1.38806	1.389481	1.40546
20	1.34078	1.34693	1.35556	1.36256	1.37077	1.379	1.38656	1.39322	1.40381
30	1.33952	1.34562	1.35418	1.3611	1.36923	1.37739	1.38494	1.39156	/
40	1.33799	1.34402	1.35273	1.35944	1.36746	1.37555	1.38307	1.38959	1.4001
50	1.33633	1.34228	1.35078	1.35759	1.36557	1.3736	1.38102	1.38765	1.3981
60	1.33429	1.34035	1.3488	1.35546	1.36425	1.3715	1.37886	1.38553	1.39609

Table S13: Refractive index n of mannitol in water. Concentration c in the mass fraction of mannitol.

	n					
c/wt T/°C	0.0218	0.0408	0.0615	0.0842	0.1035	0.1466
10	1.33729	1.33994	1.34332	1.34655	1.34963	1.35638
20	1.33647	1.33905	1.34239	1.34556	1.3486	1.35523
30	1.33526	1.33783	1.3412	1.34424	1.3473	1.35387
40	1.33373	1.33632	1.33959	1.34279	1.34576	1.35218
50	1.33205	1.33456	1.33783	1.3409	1.34386	1.35032
60	1.3301	1.33265	1.33591	1.33904	1.34194	1.34856

S3 Density and viscosity data used for the analysis

In the following we list the literature values for the density and the viscosity used in Eq.9 in the main manuscript.

S3.1 Density and viscosity for 1-propanol

According to Pang [6] the density ρ in [kg/m^3] at 25°C can be estimated within 0.2% using linear function in dependence of mass fraction c.

$$\rho(c) = (997.0 \pm 0.8) - (135 \pm 8)c - (122 \pm 20)c^2 + (62 \pm 13)c^3. \quad (1)$$

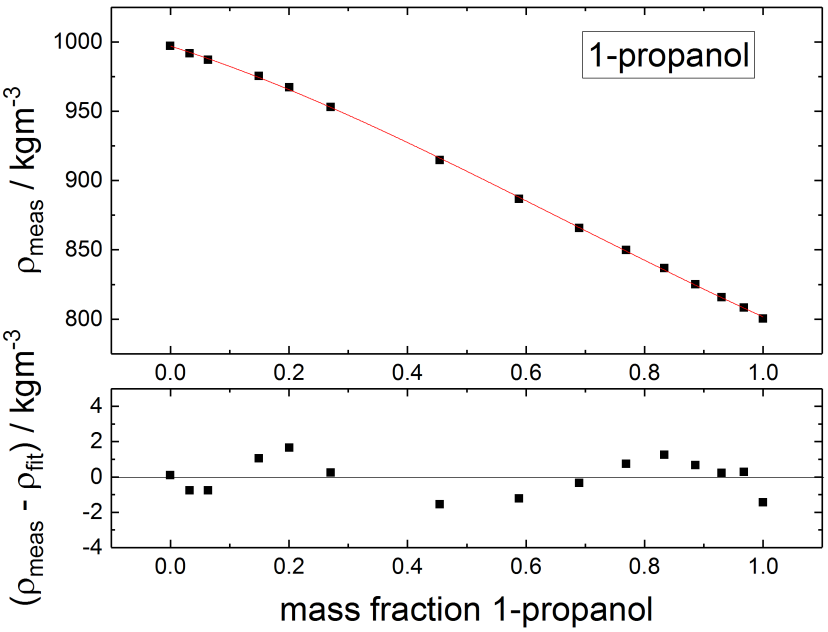

Figure S1: Density and the residuals of 1-propanol/water mixtures as function of mass fraction of 1-propanal at $T = 25$°C. The solid line is a fit according to Eq.1.

The dynamic viscosity η at 25°C can be described by a second order fit with a mean deviation of 0.04%.

$$\eta(c) = (8.50 \pm 0.26) \times 10^{-4} + (5.93 \pm 0.14) \times 10^{-3}c - (4.9 \pm 0.1) \times 10^{-3}c^2 \quad (2)$$

Table S14: Density and viscosity for 1-propanol [6] at 25°C as function of molar fraction x and mass fraction c of 1-propanol.

x	c/wt	$\rho/10^3$ kg m^{-3}	$\eta/10^{-3}$ kg m^{-1} s^{-1}
0	0	0.99705	0.890
0.01	0.03259	0.99167	1.024
0.02	0.06373	0.98712	1.160
0.05	0.14933	0.97534	1.603
0.07	0.20067	0.96711	1.844
0.1	0.27039	0.95301	2.116
0.2	0.45470	0.91461	2.598
0.3	0.58838	0.88665	2.674
0.4	0.68979	0.86571	2.592
0.5	0.76934	0.84973	2.465
0.6	0.83343	0.83668	2.333
0.7	0.88617	0.82512	2.202
0.8	0.93029	0.81568	2.097
0.9	0.96775	0.80825	2.022
1	1	0.80021	1.947

S3.2 Density and viscosity for butane-1,4-diol

According to George [7] the density of butane-1,4-diol ρ in [kg/m^3] at 25°C can be estimated within 0.2% using a third order fit dependence of mass fraction c.

$$\rho(c) = (997.4 \pm 0.1) + (27.0 \pm 0.9)c + (63 \pm 29)c^2 - (74.8 \pm 1.4)c^3 \qquad (3)$$

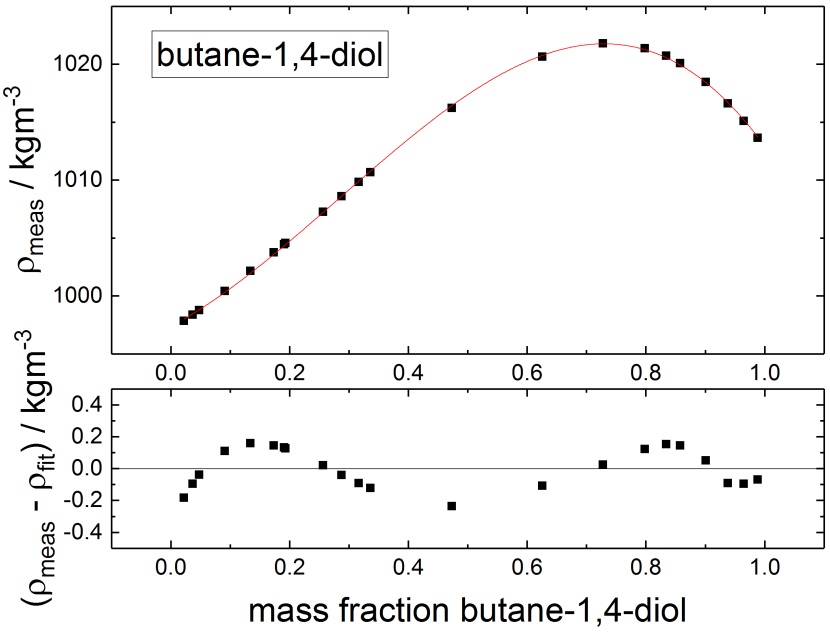

Figure S2: Density and the residuals of butane-1,4-diol/water mixtures as function of mass fraction of butane-1,4-diol at $T = 25$°C. The solid line is a fit according to Eq.3.

The dynamic viscosity η at 25°C can be described by an exponential fit with a mean deviation of 1.72%.

$$\eta(c) = (3.29 \pm 0.42) \times 10^{-4} \exp\left(\frac{c}{(0.18706 \pm 0.005)}\right) + (2.22 \pm 0.3) \times 10^{-3} \qquad (4)$$

Table S15: Density and viscosity for butane-1,4-diol [7] at 25°C. Concentration c in the mass fraction of butane-1,4-diol.

$x(H_2O)$	x	c/wt	$\rho/10^3$ kg m^{-3}	$\eta/10^{-3}$ kg m^{-1} s^{-1}
0.9955	0.0045	0.02211	0.99783	1.158
0.9924	0.0076	0.03689	0.99837	1.337
0.9901	0.0099	0.04763	0.99877	1.468
0.9804	0.0196	0.09091	1.00042	2.001
0.9699	0.0301	0.13438	1.00214	2.544
0.9597	0.0403	0.17359	1.00374	3.045
0.955	0.045	0.19075	1.00446	3.267
0.9543	0.0457	0.19325	1.00456	3.3
0.9355	0.0645	0.25644	1.00724	4.148
0.9253	0.0747	0.28766	1.00858	4.588
0.9152	0.0848	0.3167	1.00983	5.014
0.9081	0.0919	0.33609	1.01066	5.31
0.8475	0.1525	0.47371	1.01621	7.83
0.7496	0.2504	0.6256	1.02065	12.569
0.6513	0.3487	0.72812	1.02178	18.652
0.5578	0.4422	0.79861	1.02137	25.512
0.498	0.502	0.8345	1.02071	30.264
0.4531	0.5469	0.85791	1.02008	33.946
0.3542	0.6458	0.90119	1.01846	42.264
0.2472	0.7528	0.9384	1.01659	51.483
0.1534	0.8466	0.96504	1.0151	59.729
0.055	0.945	0.9885	1.01364	68.263

S3.3 Density and viscosity for propane-1,3-diol

According to George [7] the density of propane-1,3-diol ρ in [kg/m^3] at 25°C can be estimated within 0.3% using a third order fit dependence of mass fraction c.

$$\rho(c) = (997.47) + (57.26 \pm 1.31)c + (62.36 \pm 3.15)c^2 - (67.24 \pm 2.12)c^3 \quad (5)$$

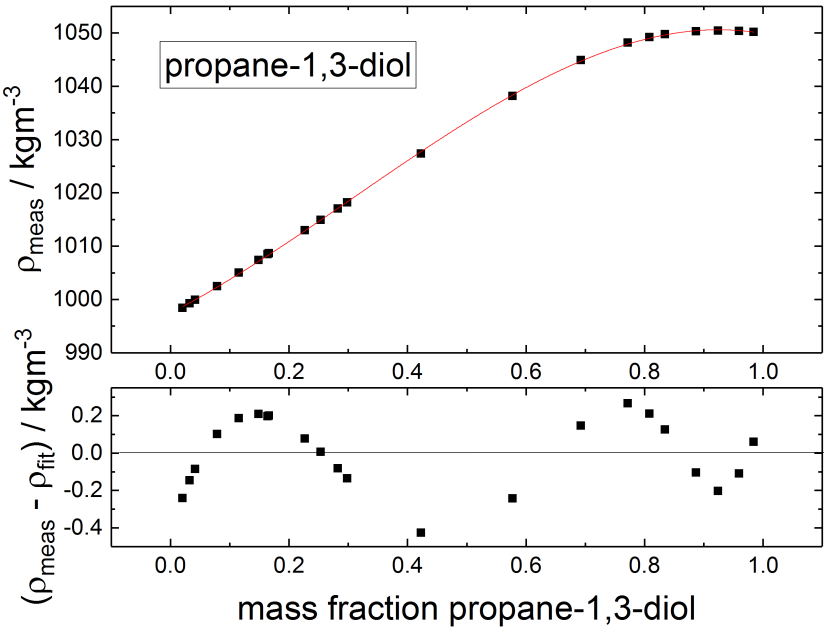

Figure S3: Density and the residuals of propane-1,3-diol/water mixtures as function of mass fraction of propane-1,3-diol at $T = 25$°C. The solid line is a fit according to Eq.5.

The dynamic viscosity η at 25°C can be described by an exponential fit with a mean deviation of 0.94%.

$$\eta(c) = (3.069 \pm 0.123) \times 10^{-4} \exp\left(\frac{c}{(0.206 \pm 0.002)}\right) + (7.756 \pm 0.595) \times 10^{-4} \quad (6)$$

Table S16: Density and viscosity for propane-1,3-diol [7] at 25°C. Concentration c in the mass fraction of propane-1,3-diol.

x_{H_2O}	x	c/wt	$\rho/10^3$ kg m^{-3}	$\eta/10^{-3}$ kg m^{-1} s^{-1}
0.9951	0.0049	0.02037	0.99842	0.939
0.9921	0.0079	0.03254	0.99925	0.971
0.9897	0.0103	0.0421	0.9999	0.997
0.9801	0.0199	0.07898	1.00245	1.107
0.97	0.03	0.11553	1.005	1.233
0.9602	0.0398	0.14898	1.00737	1.365
0.9556	0.0444	0.16404	1.00844	1.43
0.9548	0.0452	0.16662	1.00863	1.442
0.935	0.065	0.22697	1.01297	1.749
0.9255	0.0745	0.25372	1.01492	1.91
0.9147	0.0853	0.28257	1.01703	2.104
0.9085	0.0915	0.29843	1.01819	2.22
0.8522	0.1478	0.4228	1.02732	3.434
0.7553	0.2447	0.57776	1.03816	6.136
0.6522	0.3478	0.69252	1.04485	9.731
0.5548	0.4452	0.77216	1.04818	13.67
0.5	0.5	0.80856	1.04921	16.068
0.4555	0.5445	0.83467	1.04974	18.092
0.35	0.65	0.88692	1.0503	23.093
0.2563	0.7437	0.92456	1.05038	27.677
0.1496	0.8504	0.96001	1.05032	32.924
0.0622	0.9378	0.98454	1.05019	37.147

S3.4 Density and viscosity for ethane-1,2-diol

According to Tsierkezos [8] the density of ethane-1,2-diol ρ in [kg/m^3] at 25°C can be estimated within 0.03% using a third order fit dependence of mass fraction c.

$$\rho(c) = (997.21) + (118.21 \pm 2.97)c + (48.879 \pm 7.083)c^2 - (55.75 \pm 4.65)c^3 \quad (7)$$

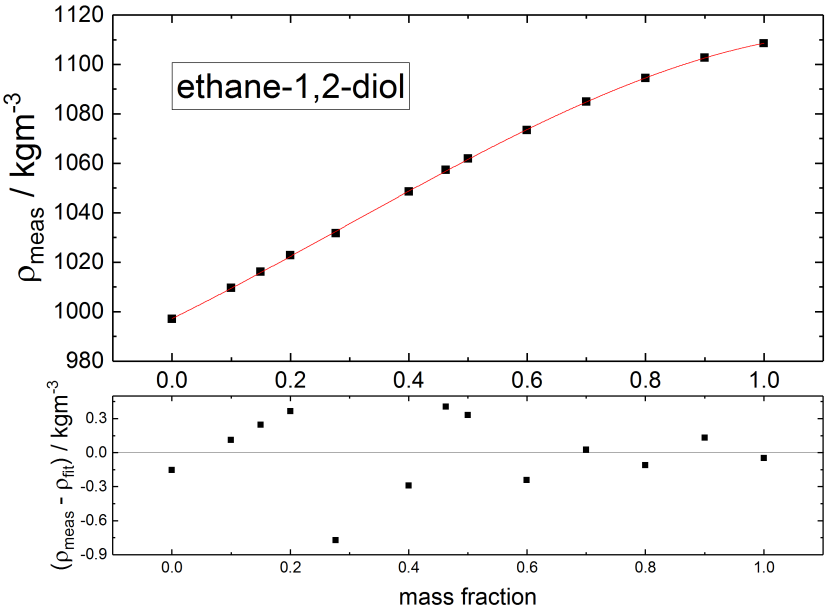

Figure S4: Density and the residuals of ethane-1,2-diol/water mixtures as function of mass fraction of ethane-1,2-diol at $T = 25$°C. The solid line is a fit according to Eq.7.

The dynamic viscosity η at 25°C can be described by an exponential fit with a mean deviation of 0.36%.

$$\eta(c) = (3.167 \pm 0.303) \times 10^{-4} \exp\left(\frac{c}{-(0.255 \pm 0.006)}\right) + (7.731 \pm 0.984) \times 10^{-4} \quad (8)$$

Table S17: Density and viscosity for ethane-1,2-diol [8] at 25°C. Concentration c in the mass fraction of ethane-1,2-diol.

x	c/wt	$\rho/10^3$ kg m^{-3}	$\eta/10^{-3}$ kg m^{-1} s^{-1}
0.0000	0.00000	0.99706	0.899
0.0312	0.09987	1.00956	1.14
0.0487	0.14993	1.01609	1.3
0.0677	0.20012	1.02274	1.47
0.1	0.27683	1.03172	1.76
0.1622	0.40012	1.04847	2.42
0.2	0.46275	1.05725	2.86
0.225	0.50006	1.0619	3.17
0.303	0.59964	1.0734	4.17
0.4038	0.70001	1.08481	5.73
0.5373	0.80003	1.0944	8.00
0.7232	0.90002	1.10268	11.31
1	1	1.10849	16.98

S3.5 Density and viscosity for arabitol

According to Zhu [9] the density of arabitol ρ in [kg/m^3] at 25°C can be estimated within 0.05% using a third order fit dependence of mass fraction c.

$$\rho(c) = (997.27 \pm 0.01) + (326 \pm 3)c + (114 \pm 46)c^2 - (33 \pm 188)c^3 \qquad (9)$$

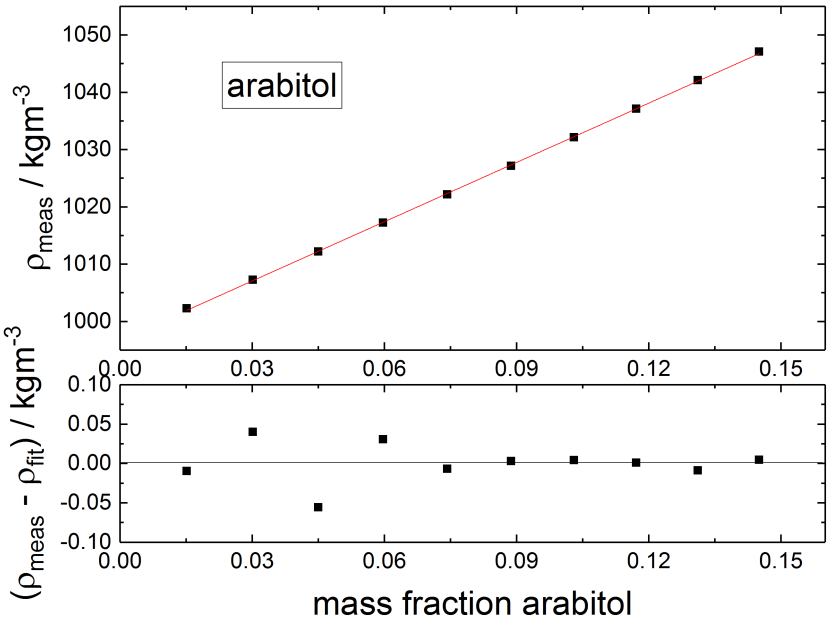

Figure S5: Density and the residuals of arabitol/water mixtures as function of mass fraction of arabitol at $T = 25$°C. The solid line is a fit according to Eq.9.

The dynamic viscosity η at 25°C can be described by an exponential fit with a mean deviation of 0.01%.

$$\eta(c) = (2.755 \pm 0.498) \times 10^{-4} \exp\left(\frac{c}{0.156 \pm 0.018}\right) + (6.463 \pm 0.544) \times 10^{-4} \qquad (10)$$

Table S18: Density and viscosity for arabitol [9] at 25°C. Concentration c in the mass fraction of arabitol.

c/mol dm^{-3}	c/wt	$\rho/10^3$ kg m^{-3}	$\eta/10^{-3}$ kg m^{-1} s^{-1}
0.1	0.01516	1.00223	0.95601
0.2	0.03017	1.00725	0.97644
0.3	0.04504	1.01213	1.01275
0.4	0.05975	1.01719	1.04849
0.5	0.07432	1.02213	1.08674
0.6	0.08875	1.02712	1.12942
0.7	0.10303	1.0321	1.18609
0.8	0.11718	1.03708	1.23221
0.9	0.13118	1.04205	1.29042
1	0.14506	1.04705	1.33862

S3.6 Density and viscosity for mannitol

According to Zhu [9] the density of mannitol ρ in [kg/m^3] at 25°C can be estimated within 0.05% using a third order fit dependence of mass fraction c.

$$\rho(c) = (997.2 \pm 0.1) + (345 \pm 5)c - (27 \pm 68)c^2 - (461 \pm 284)c^3 \qquad (11)$$

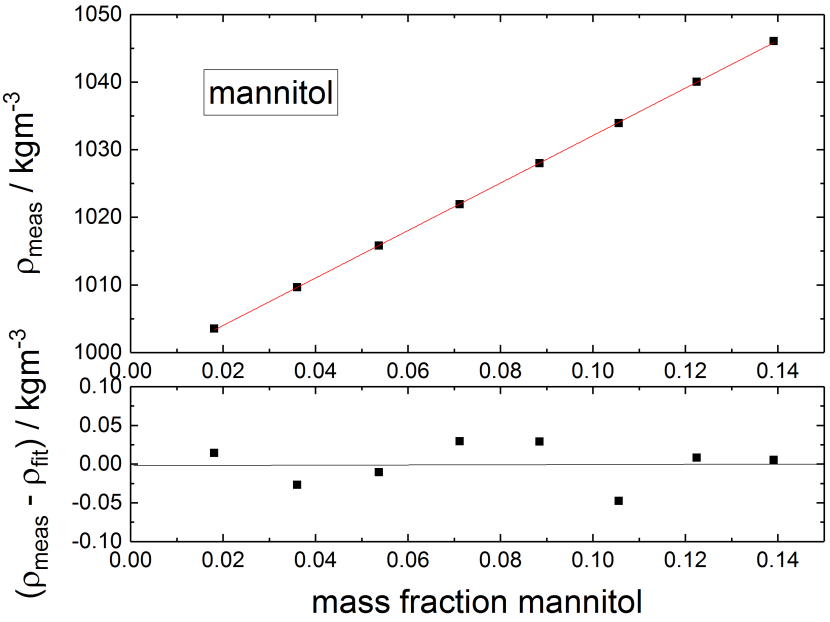

Figure S6: Density and the residuals of mannitol/water mixtures as function of mass fraction of mannitol at $T = 25$°C. The solid line is a fit according to Eq.11.

The dynamic viscosity η at 25°C can be described by an exponential fit with a mean deviation of 0.01%.

$$\eta(c) = (0.925) + (2.894 \pm 0.185)c + (3.007 \pm 1.145)c^2 \qquad (12)$$

Table S19: Density and viscosity for mannitol [9] at 25°C. Concentration c in the mass fraction of mannitol.

c/mol dm^{-3}	c/wt	$\rho/10^3$ kg m^{-3}	$\eta/10^{-3}$ kg m^{-1} s^{-1}
0.1	0.01813	1.00351	0.97604
0.2	0.03604	1.00965	1.03547
0.3	0.05374	1.01579	1.09011
0.4	0.07123	1.02191	1.15283
0.5	0.08851	1.02796	1.20234
0.6	0.10559	1.03392	1.25982
0.7	0.12247	1.04001	1.3224
0.8	0.13915	1.04605	1.39013

S4 Thermal diffusion coefficient

In the main manuscript we discuss and show the Soret coefficient S_T and the diffusion coefficient D as function of temperature for the investigated alcohols. For completeness we add here also the thermal diffusion coefficient D_T. The thermal diffusion coefficient of 1-propanol is larger than the D_T-values of the other alcohols and the temperature dependence is different. The thermal diffusion coefficient of 1-propanol seems to approach a constant value at higher temperatures, while the other systems show a linear or parabolic increase of D_T with increasing temperature. As discussed in the main manuscript this is probably related to the cluster formation.

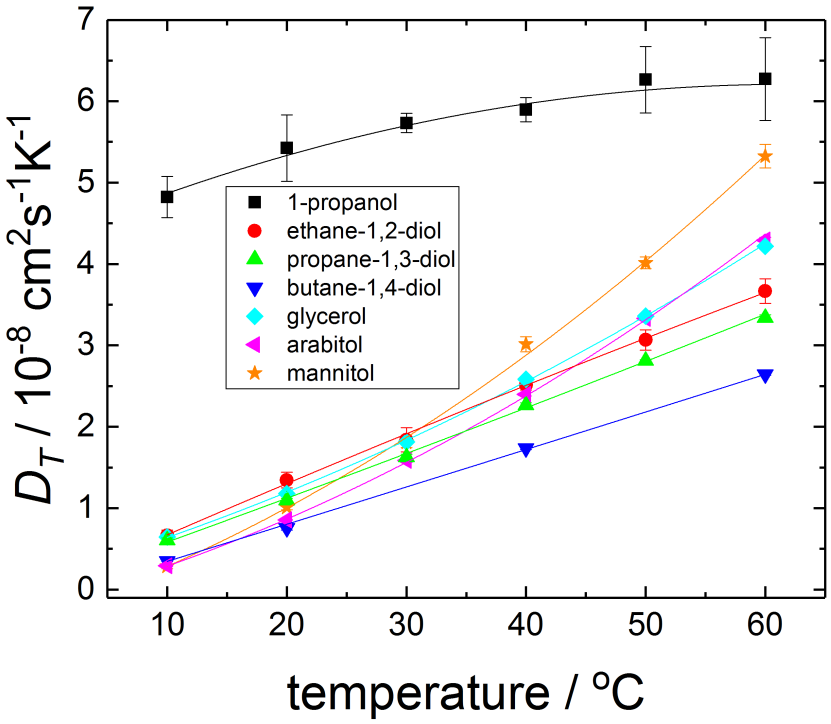

Figure S7: Thermal diffusion coefficient of 1-propanol, ethylene glycol, glycerol, propane-1,3-diol, mannitol, arabitol and butane-1,4-diol as function of temperature. Except for 1-propanol with a weight fraction of 0.1 the weight fraction of the alcohols was 0.25. The same symbols as in figure 1 are used.

S5 Partition coefficient

Table S20 lists the log$P$-values calculated using calculator Plugins of Marvin 16.5.2.0 for all systems displayed in figure 6 in the main manuscript.

Table S20: Used log$P$-values of sugars[10, 11], cyclodextrins[12], amides[13], aspirin[14] and ethanol[15].

Compounds	log$P$	$\Delta S_{\mathrm{T}} = S_{\mathrm{T}}(50°\mathrm{C}) - S_{\mathrm{T}}(20°\mathrm{C})$ / K^{-1}
α-CD	−12.7	0.00624
β-CD	−14.82	0.00716
γ-CD	−16.93	0.007
aspirin	1.06	-0.0026
glucose	−4	0.00216
sucrose	−4.87	0.0033
cellobiose	−5.38	0.00323
maltose	−5.38	0.0032
melezitose	−6.99	0.00382
rafinose	−6.99	0.00428
stachyose	−9.1	0.00496
urea	−1.3	7.8495E-4
formamide	−1.13	1.832E-4
acetamide	−1.03	-7.43333E-4
methylformamide	−0.89	-6.81667E-4
dimethylformamide	−0.64	-0.00116
ethanol	−0.16	-0.00247
1-propanol	0.24	-0.00378
ethane-1,2-diol	−1.31	2.1E-4
propane-1,2-diol	−0.9	-6.4E-4
propane-1,3-diol	−1.26	3.5725E-4
butane-1,4-diol	−0.81	5E-4
glycerol	−1.98	6.685E-4
arabitol	−3.33	0.00154
mannitol	−4	0.00188

S6 Diffusion coefficient calculations

Table S22 lists the measured and the calculated diffusion coefficients D_{Evans} and $D_{\mathrm{W\&C}}$ according to equations 9 and 3 in the main manuscript.

Table S22: Measured and calculated diffusion coefficient (using 9) of 1-propanol, ethylene glycol, propane-1,3-diol, butane-1,4-diol, glycerol and arabitol.

alcohol	c/ wt	$D_{\mathrm{meas.}}$/ $10^{-6}\mathrm{cm}^2\ \mathrm{s}^{-1}$	D_{Evans}/ $10^{-6}\mathrm{cm}^2\ \mathrm{s}^{-1}$	$D_{\mathrm{W\&C}}$/ $10^{-6}\mathrm{cm}^2\ \mathrm{s}^{-1}$
Mannitol	0.11	5.58	5.71	6.66
Arabitol	0.107	6.30	6.63	7.90
Glycerol	0.12	8.49	8.71	10.05
Ethylene glycol	0.272	7.91	6.91	7.73
Propane-1,3-diol	0.12	7.83	8.23	8.80
Butane-1,4-diol	0.263	4.74	2.86	2.93
1-propanole	0.108	6.69	8.45	7.93

References

[1] Gerardino D'Errico, Ornella Ortona, Fabio Capuano, and Vincenzo Vitagliano. Diffusion coefficients for the binary system glycerol + water at 25 °C. a velocity correlation study. *J. Chem. Eng. Data*, 49(6):1665–1670, 2004.

[2] A. Bondi. van der waals volumes and radii. *J. Phys. Chem.*, 68(3):441–451, 1964.

[3] A. Becker, W. Köhler, and B. Müller. A scanning michelson interferometer for the measurement of the concentration and temperature derivative of the refractive- index of liquids. *Ber. Bunsen-Ges. Phys. Chem. Chem. Phys.*, 99:600–608, 1995.

[4] Rafael D. Camerini-Otero, Richard M. Franklin, and Loren A. Day. Molecular weights, dispersion of refractive index increments, and dimensions from transmittance spectrophotometry. bacteriophages r17, t7, and pm2, and tobacco mosaic virus. *Biochemistry*, 13:3763–3773, 1974.

[5] V. V. Sechenyh, J. C. Legros, and V. Shevtsova. Experimental and predicted refractive index properties in ternary mixtures of associated liquids. *J. Chem. Thermodyn.*, 43:1700–1707, 2011.

[6] Fong-Meng Pang, Chye-Eng Seng, Tjoon-Tow Teng, and M. H. Ibrahim. Densities and viscosities of aqueous solutions of 1-propanol and 2-propanol at temperatures from 293.15k to 333.15k. *J. Mol. Liq.*, 136:71–78, 2007.

[7] John George and Nandhibatla V. Sastry. Densities, dynamic viscosities, speeds of sound, and relative permittivities for water + alkanediols (propane-1,2- and -1,3-diol and butane-1,2-, -1,3-, -1,4-, and -2,3-diol) at different temperatures. *J. Chem. Eng. Data*, 48(6):1529–1539, 2003.

[8] N. G. Tsierkezos and I. E. Molinou. Thermodynamic properties of water plus ethylene glycol at 283.15, 293.15, 303.15, and 313.15 k. *J. Chem. Eng. Data*, 43:989–993, 1998.

[9] Chunying Zhu, Youguang Ma, and Chuanling Zhou. Densities and viscosities of sugar alcohol aqueous solutions. *J. Chem. Eng. Data*, 55(9):3882–3885, 2010.

[10] Pablo Blanco, Hartmut Kriegs, Bastian Arlt, and Simone Wiegand. Thermal diffusion of oligosaccharide solutions: The role of chain length and structure. *The Journal of Physical Chemistry B*, 114(33):10740–10747, 2010.

[11] Pablo Blanco and Simone Wiegand. Study of the soret effect in monosaccharide solutions. *The Journal of Physical Chemistry B*, 114(8):2807–2813, 2010.

[12] Kazuya Eguchi, Doreen Niether, Simone Wiegand, and Rio Kita. Thermophoresis of cyclic oligosaccharides in polar solvents. *Eur. Phys. J. E*, 39:86, 2016.

[13] D. Niether, H. Kriegs, J. K. G. Dhont, and S. Wiegand. Peptide model systems: Correlation between thermophilicity and hydrophilicity. *J. Chem. Phys.*, 149, 2018.

[14] D. Niether, T. Kawaguchi, J. Hovancova, K. Eguchi, J. K. G. Dhont, R. Kita, and S. Wiegand. Role of hydrogen bonding of cyclodextrin-drug complexes probed by thermodiffusion. *Langmuir*, 33:8483–8492, 2017.

[15] A. Königer, B. Meier, and W. Köhler. Measurement of the soret, diffusion, and thermal diffusion coefficients of three binary organic benchmark mixtures and of ethanol-water mixtures using a beam deflection technique. *Philos. Mag.*, 89:907–923, 2009.